6

Colour simulation of textiles

H SHEN AND J H XIN, The Hong Kong Polytechnic University, Hong Kong

6.1 Introduction

Colour is one of the most important aspects for the textile and garment industry. In colour design and colour quality control, visualisation of solid colours on display devices has become a routine process for many companies. These solid colours are firstly measured using a spectrophotometer and are then displayed on a monitor. When properly calibrated and characterised, the monitor can display the colour of the physical sample with very high accuracy. A spectrophotometer measures the average colour in a fixed aperture, regardless of the spatial variation of the colour. As a consequence, it is possible that two textile fabrics with different visual colour appearance may have the same measurement result. In addition, when textile fabrics are heavily textured, their colours cannot be regarded as solid colours and therefore visualisation using solid colour is not suitable for heavily textured fabric samples. There is a need to map solid colours to various texture patterns and this colour mapping technique should generate a textured colour image accurately so that it is perceptually very close to the original image and/or physical textile fabric samples. Colour simulation of texture images also has other advantages such as visualisation of the yarn-dyed fabrics before they are actually produced. In addition to the two-dimensional textile fabrics, there is also a need for the colour synthesis of three-dimensional textile products. For example, in a virtual exhibition of textile products or interior design, it is always desirable to change the colour of three-dimensional objects to obtain different visual effects.

Image synthesis is an important research area in computer graphics, and methods including texture synthesis and colour transfer have been studied recently. The goal of image synthesis in computer graphics is to create photo-realistic images, without special consideration of colour accuracy. In textile applications, however, the colour fidelity is a very important issue. It is generally accepted that the pass and fail tolerance for textile fabrics is

about 0.6 to 1.0 CIELAB colour difference unit. For heavily textured colour samples, the visual tolerance may become larger due to the parametric effect of texture.[1] Colour accuracy is also very important in the colour synthesis of three-dimensional products, as colour appearance is one of the major factors that affect customer appreciation.

In this chapter, the colour mapping algorithm for a two-dimensional textile fabric image is first introduced, and then the texture effect on visual colour difference evaluation is investigated. This is followed by the colour synthesis technique for three-dimensional textile products, which is based upon a physical vision model. Finally, future trends in colour simulation are discussed and further information in this area is provided.

6.2 Characterisation of colour displays

In the textile industry, colour cathode-ray tubes (CRTs) are widely used for the visualisation of solid colours. To ensure that the colour displayed is the same as that of the physical sample, the CRTs must be characterised. Characterisation of a computer-controlled CRT display is to establish the relationship between the digital signals and the output visual stimuli. The input signals are typically the digital-to-analogue converter (DAC) pixel values, denoted as RGB, and the output stimuli are the measured CIE tristimulus values such as XYZ. The gain-offset-gamma (GOG) model is the most well-known mathematical method for characterisation, and it is also the method recommended by CIE.[2,3] The characterisation consists of two stages, as shown in Fig. 6.1.

Stage one is a one-dimensional non-linear transformation for each channel from RGB to the output luminance levels $L_R L_G L_B$, which is known as gamma correction in the GOG model. Stage two is a linear, three-dimensional transformation from luminance $L_R L_G L_B$ to tristimulus values XYZ using a 3×3 matrix. To calculate the parameters in the GOG model, the luminances and chromaticities of the three primaries, white and black points, and a series of neutral scales needs to be measured.

Recently, flat-panel liquid-crystal displays (LCDs) have become more and more popular in various applications and eventually they may replace all CRTs. LCDs are superior to CRTs in terms of luminance, contrast ratio, sharpness and spatial uniformity, while its main deficiency is the view angle dependencies. The characterisation of LCD is similar to that of CRT, with the exception that the linearisation is accomplished by one-dimensional look-up tables.[4]

6.1 The two-stage characterisation of displays.

6.3 Colour mapping for two-dimensional texture image

Texture and colour are two important characteristics of images.[5] Given an original texture image and a solid target colour, the purpose of colour mapping is to simulate a new colour texture image that is a close replica of the target image. With the technique of colour mapping, the final styles of textured textile fabrics could be visualised before they were actually produced. In the literature, Botchko *et al.*[6] analysed the relationship between the mean spectral and standard deviation of natural objects, and proposed parametric methods for the virtual colourisation of texture image. Montag and Berns also presented a method to simulate textile colour texture image in CIELCH colour space, using a singular value decomposition technique.[7] In this section, a computational model for colour mapping on a textile texture image, considering colour fidelity, is presented. Using this model, the colour accuracy in texture image simulation can be improved.

Texture images were scanned in using an Epson GT-10000+ flatbed colour image scanner. The physical textile samples are cotton fabrics with different woven patterns. Samples of each of the woven patterns were dyed into several colours, including green, orange, purple, pink and turquoise using reactive dyestuffs. These textile fabrics were then scanned in a resolution that gave approximately equal visual appearances to those of the physical samples when viewed under normal viewing distance of about 25 to 30 cm. Some texture images of these textile fabrics are shown in Fig. 6.2.

6.3.1 Analysis of texture image characteristics

The RGB space directly corresponds to the output of imaging devices, such as colour scanner and digital camera. Let $L(\lambda; p)$ refer to the spectral distribution function of light entering the imaging device at pixel position p, and $s_n(\lambda)$ be the spectral sensitivity of the nth sensor. The output signal becomes:

$$V_n^p = \int L(\lambda; p) s_n(\lambda) \mathrm{d}\lambda \qquad [6.1]$$

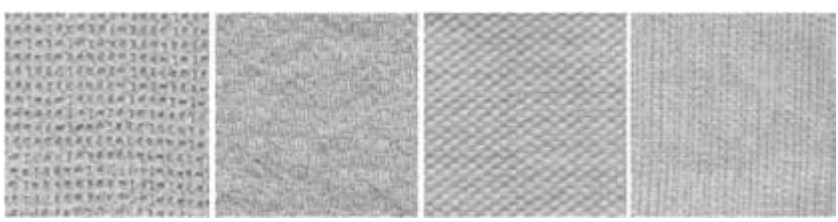

6.2 Four textile fabric samples with different texture patterns.

It should be noted that (eqn 6.1) assumes that the output of the imaging device is proportional to the light intensity entering the sensor. The luminance channel contains mainly the texture information, and can be calculated according to:

$$Y^p = 0.299V_1^p + 0.587V_2^p + 0.114V_3^p \quad [6.2]$$

The histograms of the red, green, blue and luminance channels (yellow) of a typical texture image are shown in Fig. 6.3 (see also colour section). The shapes of the histograms in different channels are similar, with differences only in height and width. However, the histogram only demonstrates the global statistical distribution of each channel. To simulate a texture image at the pixel-wise scale, the spatial distribution should be analysed. The correlation between the RGB and the luminance channels can be investigated using the pixel deviations to the mean value in RGB channel and luminance channel, as shown in Fig. 6.4. The degree of correlation can be described using the correlation coefficient. For a perfect correlation, the correlation coefficient should be equal to 1.0. The correlation coefficient of the blue channel, 0.988, is the highest, followed by that of the red channel, 0.985. The correlation coefficient of the green channel, 0.915, is the lowest. This observation indicates the existence of high channel correlation of texture images.

6.3.2 Colour mapping algorithm

The colour mapping algorithm assumes that only the spatial distribution of the luminance channel is known, and the purpose of the algorithm is to derive three-dimensional spatial distributions of the red, green and blue channels from a one-dimensional channel. This problem is therefore undetermined since the combination of different V_n^p values can produce the same Y^p value (see eqn 6.2). From the constraint of channel correlation,

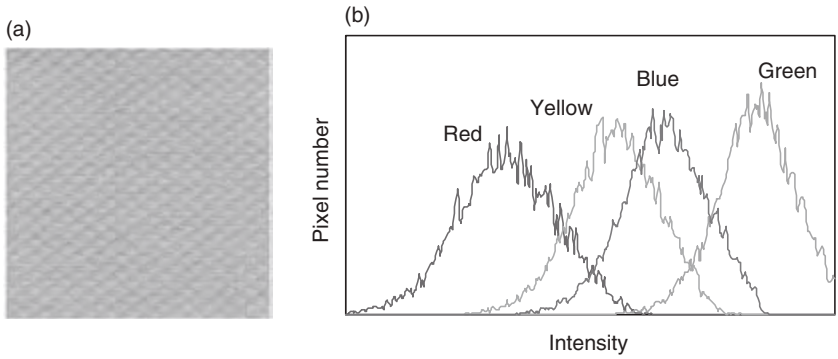

6.3 (a) A typical texture image, (b) its histograms of different channels.

a solution can be found so that the synthesised texture image is perceptually close to the target one. That is, the overall colour difference between the generated and actual image is very small.

Let S_n be the user-specified target colour in RGB space. Then, the generated colour at pixel p can be simply calculated as

$$U^p{}_n = S_n + \Delta Y^p \qquad [6.3]$$

where ΔY^p is the pixel deviation to mean luminance. For instance, if the selected target colour is (100,150,200), and for a particular pixel p, ΔY^p = 10, then, for that pixel, the new colour becomes (110,160,210). When $U^p{}_n$ is smaller than 0 or larger than 255, it should be clipped to 0 and 255, respectively.

The colour mapping algorithm according to (eqn 6.3) is simplified, as it assumes the pixel deviations in RGB channels are exactly the same as that in the luminance channel. For texture images, it is not the case (see Fig. 6.4, also in colour section). By taking the standard deviation of the colour channel into consideration, the colour mapping algorithm becomes

$$U^p{}_n = S_n + \left(\frac{\sigma_n}{\sigma_Y}\right)\Delta Y^p \qquad [6.4]$$

where σ_n is the standard deviation of the nth channel of the generated texture image, and σ_Y is the standard deviation of the luminance channel. For texture images of textile fabrics, it is found that the standard deviation is always related to the mean colour.[8,9] Therefore, it is possible to calculate the σ_n value for a given target colour using their relationship. Alternatively, the

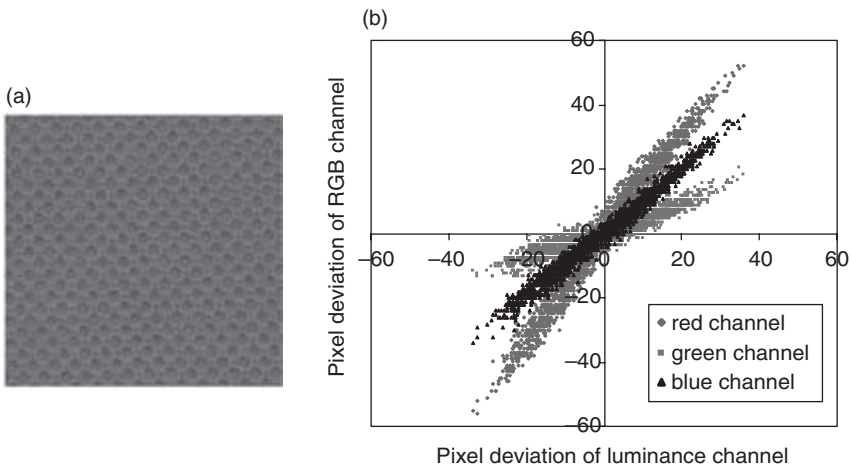

6.4 (a) Texture image, (b) relationship between pixel deviation in luminance channel and that in RGB channels.

value of σ_n can also be specified by the user if he/she wants to learn the visual appearance of the synthesised image under different texture strengths.

6.3.3 Colour mapping results and discussions

Some experimental results are shown in Fig. 6.5 (see also colour section). To evaluate the colour accuracy of the algorithm, we use the mean colour of the original image as a target colour to generate a new texture image. The colour scanner was characterised and the RGB value of each pixel was then transformed into a device-independent CIEXYZ value. Then, colour differences ΔE^*_{ab} between the original and generated image were calculated on a pixel-wise scale, as shown in Fig. 6.6.

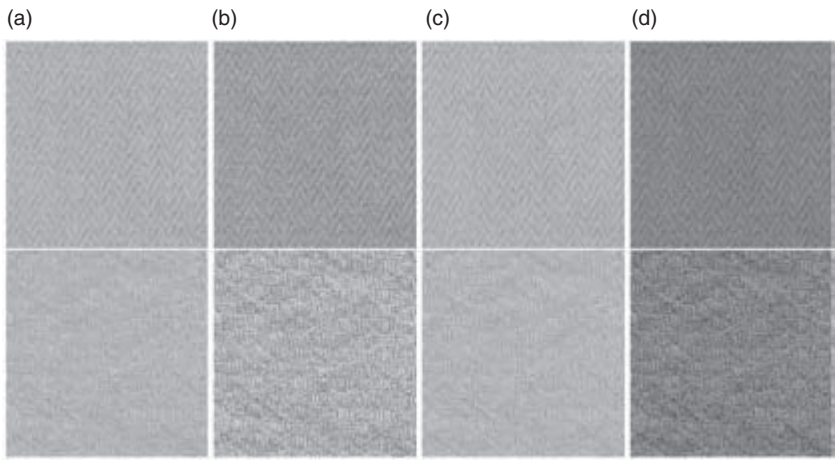

6.5 Experimental results of colour mapping algorithm. (a) original, (b) luminance channel, (c) colour mapping using the mean colour of the original image as target colour, (d) colour mapping using another target colour.

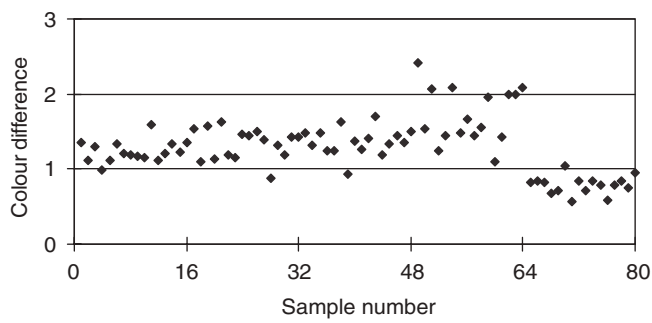

6.6 Average pixel-wise colour difference between the original and generated image.

It was reported that the threshold for detecting the colour difference of a pair of solid colour samples is around 1.0 unit of ΔE^*_{ab} colour difference. Nevertheless, in the case of colour with texture, one can hardly perceive the difference between the original image and the generated one even if the mean colour difference is 1.29, as shown in this study. This result is attributable to the parametric effect of the texture.

6.4 Texture effect on visual colour difference evaluation

It is known that texture has an important effect on colour perception, as a parametric factor to the colour difference equations. However, few reports on quantitative analysis of the influence have been published. A lightness tolerance thresholds experiment was performed by Montag and Berns[7] using the stimuli with a simulated texture of thread wound on a card. They found that the textured stimuli had the effect of increasing the tolerance thresholds by a factor of almost 2, when compared with uniform stimuli. In this section, the influence of texture levels on visual colour difference is evaluated by using 15 samples with different texture patterns. These textured colour samples were first generated using a colour mapping algorithm, together with five pre-determined colour centres, and then displayed on a characterised cathode ray tube (CRT) monitor. For each texture pattern, two comparison pairs (with ±5 lightness difference) were used, and thus a total of 150 (15 samples × 5 colour centres × 2 pairs) colour difference pairs were evaluated using the grey-scale method.

6.4.1 Texture characterisation using histogram half-width

For textile fabric, the texture is quite regular, that is, the elementary woven or knitted pattern is repeated over the whole image. The texture level can be described by its coarseness index in the sense that a rhomb fabric is coarser than a plain one under the same viewing conditions. The coarseness index is related to the spatial repetition period of the local structure. A large repetition period implies a coarse texture, while a small period implies a fine one. Due to the regularity of the texture patterns of textile fabrics, the coarseness index is considered to be effective for quantitative measurement of texture level. The shape of the histogram is directly related to the coarseness of a texture, i.e. the width of coarse texture is wider than that of fine texture. Although the histogram only describes the statistical distribution of the luminance channel of the texture image, it is quite effective in characterizing the regular texture of textile fabric.

The half-width W_Y of a histogram in the luminance channel can be used to quantify the coarseness of a texture, which is called texture strength here. Suppose the luminance Y_C contains a maximum pixel number V, the half-

width W_Y is defined as the distance between the higher luminance Y_R and lower luminance Y_L containing *V/2* pixel number:

$$W_Y = Y_R - Y_L \quad [6.5]$$

Figure 6.7 illustrates the definition of texture strength in a luminance channel.

6.4.2 Colour difference pairs and visual assessment

Five colour centres were selected based on the findings whose colorimetric values are shown in Table 6.1. These colour centres were converted to display RGB space according to the gain-offset-gamma model.[2,3] For each colour centre, 30 colour mapped texture image pairs were generated, two pairs for each of the 15 textures. A spectroradiometer was used to measure the colour difference of the textured colour pairs. The distance between the spectroradiometer and the displayed texture image was about 40 cm and the average colour of a relatively large area was measured.

It is known that the human visual system is more sensitive to luminance contrast than to chromatic contrast.[10] Therefore, the texture effect was investigated on a medium colour difference of about 5.0 CIELAB units in lightness direction. This range is also on the borderline of the CIE recom-

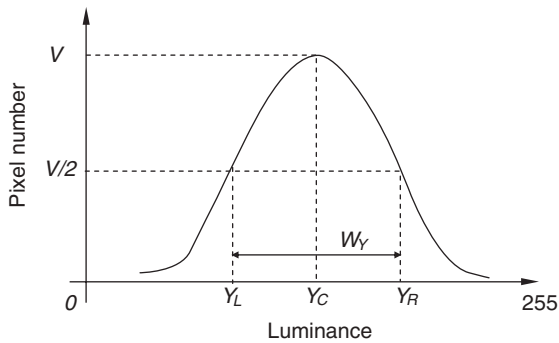

6.7 Definition of texture strength W_Y.

Table 6.1 Colour centres used in the visual colour difference evaluation

	Orange	Yellow	Grey	Green	Blue
L*	48.33	69.28	68.25	28.69	28.96
a*	13.14	4.48	3.21	–17.83	4.43
b*	16.87	19.11	0.29	–0.50	–9.13

mended colour difference magnitude for applying CIE94.[11] The target solid colours were fine tuned until the generated textured colour pairs had ±5.0 lightness differences when measured using a spectroradiometer.

The grey-scale comparison method was adopted, considering its wide use in assessing colour change in the textile industry. Five grey-scales according to the ISO standard[12] were used in the evaluation. The experiment was conducted in a completely dark room and, thus, the influence of ambient illumination was eliminated. The arrangement of grey-scales and a textured pair (or solid pair) on a CRT monitor is shown in Fig. 6.8 (see also colour section). The size of the displayed samples, including the grey-scales, was 3 inches square. All the samples displayed had no black frame and there was no dividing line between the pairs. In total, ten observers were asked to rate the colour difference using the solid colour grey-scale grades. The viewing distance is the same as that of a spectroradiometer and the viewing angle is 0° to the normal of the sample. At the beginning of each assessment, the right patch of the grey-scale pair was the same as the left one (standard). When the observer clicked one grey patch on top, the right patch of the grey-scale pairs changed to that grey. Observers were asked to give a grey-scale grade that produced approximately the same colour difference as the comparison pair. If the grade of a sample pair did not equal the grade of the closest grey-scale, observers were encouraged to provide an intermediate step. In order to evaluate the texture effect, a reference experiment, using solid colour difference pairs with the same measured colour difference as the texture mapped pairs, was also conducted under the same viewing condition.

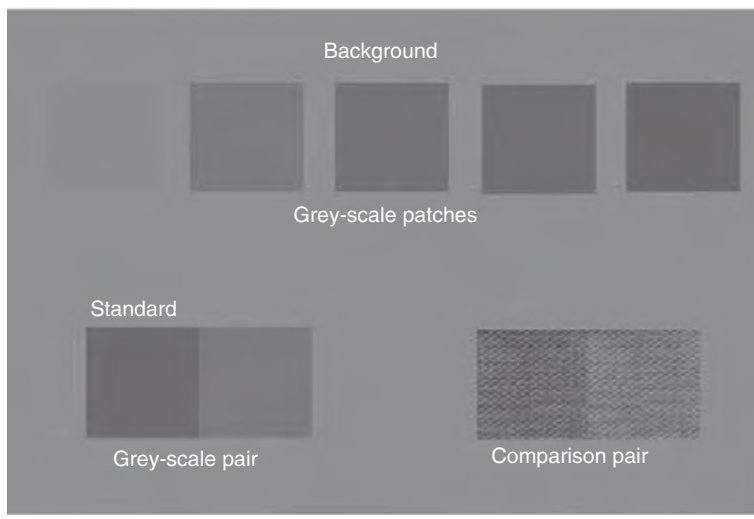

6.8 Arrangement of sample pairs and grey scales on a CRT monitor.

It is known that the reliability of the results is critical in psychophysical experiments. The observer accuracy and repeatability tests were employed to check the reliability of the results. Observer accuracy represents the average deviation between each individual and the mean visual result of a panel, while observer repeatability represents the variation of the visual assessment of a particular observer. The performance factor $(PF/3)$[11,13] has been widely used as an indicator for the observer accuracy and repeatability and for the performance of colour difference formulae in comparison with visual results. A *PF/3* combines three measures of fit: gamma factor γ, coefficient of variation *CV* and V_{AB}. The calculation of *PF/3* is given as

$$PF/3 = 100[(\gamma - 1) + V_{AB} + CV/100]/3 \quad [6.6]$$

A low *PF/3* value indicates a small difference between two variables. In the experiment, ten observers were asked to assess each textured and solid colour pairs twice. The observer accuracy and repeatability were 26.7 and 32.1, respectively. Considering these values are acceptable, all of the ten observers' results were used.

6.4.3 Visual evaluation results and discussions

The grey-scale results were converted to the visual difference ΔV according to a third-order polynomial conversion equation derived using the five grey scales. Let $\Delta V^{+}_{t,W}$ and $\Delta V^{-}_{t,W}$ be the visual difference of textured colour pairs of strength W_Y, with an increase and decrease of 5.0 units ΔE^{*}_{ab} in lightness scale, the average visual difference $\Delta V_{t,W}$ is

$$\Delta V_{t,W} = \frac{1}{2}(\Delta V^{+}_{t,W} + \Delta V^{-}_{t,W}) \quad [6.7]$$

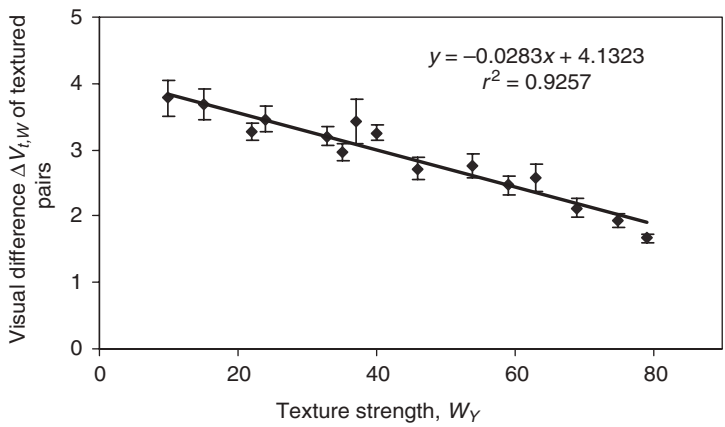

6.9 Visual difference $\Delta V_{t,W}$ against texture strength W_Y for the orange colour centre. The *y*-error bars show ±1 standard deviations.

Very high correlation was found between the visual difference $\Delta V_{t,W}$ and the texture strength W_Y for the five colour centres used. Figure 6.9 shows the relationship between $\Delta V_{t,W}$ and W_Y of the orange colour centre. Relationships of other colour centres are similar.

Let K_W be the ratio between the visual difference of a textured colour pair with strength W_Y and that of a solid colour pair:

$$K_w = \frac{1}{2}\left(\frac{\Delta V^+_{tw}}{\Delta V^+_s} + \frac{\Delta V^-_{tw}}{\Delta V^-_s}\right) \quad [6.8]$$

where ΔV^+_s and ΔV^-_s are the visual differences of the solid colour pairs with an increase and decrease of 5.0 in lightness with respect to the colour centre. The K_W value deviating from 1.0 indicates a parametric effect. The relationships between K_W and texture strength W_Y for the orange colour centre is shown in Fig. 6.10. When the half-width of the Y channel W_Y is very low, which indicates low texture strength, the K_W value is closer to 1.0. However, when W_Y increases, the K_W value becomes smaller, indicating a stronger parametric effect.

Figures 6.9 and 6.10 clearly show that the simple linear fitting could successfully reveal the texture effect on visual difference evaluation. The slope D value of the fitting line can be used to further quantify the variation of visual difference with respect to texture strength. In Table 6.2, it is found that the D values for the five colour centres are quite close. The quantitative analysis found that every increase of 10 units in texture strength in luminance scale will cause a 0.25 decrease of visual difference, and a 0.05 decrease of K_W value. Based on these fundamental quantitative results, it is possible to introduce the parametric effect of the texture effect

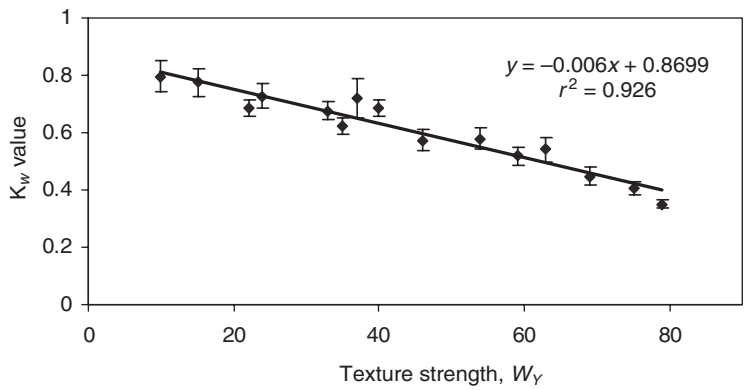

6.10 K_W value against texture strength W_Y for the orange colour centre. The *y*-error bars show ±1 standard deviation.

Table 6.2 Slope of fitting line of visual difference $\Delta V_{t,W}$ and K_W value with texture strength W_Y

	Orange	Yellow	Grey	Green	Blue
Slope of $\Delta V_{t,W}$	–0.0283	–0.0271	–0.0231	–0.0232	–0.0263
Slope of K_W	–0.0060	–0.0054	–0.0049	–0.0050	–0.0059

into a colour difference equation as a scale factor related to texture level, provided more attributes of colour differences are investigated.

This section presents the fundamental investigation of the texture effect on the visual colour difference evaluation. It is noted that two different texture images may have the same histogram, as the histogram ignores the spatial distribution of images. Therefore, it may be desirable to use additional textural features such as coarseness, contrast, busyness and complexity to represent the visual properties of texture. It should also be pointed out that consideration of the colour difference only in the lightness direction is not sufficient for practical applications, since chroma and hue may also be influenced by the texture effect.

6.5 Colour synthesis for three-dimensional objects

In computer graphics, to create a realistic image, a complete model or description of the reflectance is needed for each of the reflective objects in the scene. It is difficult to establish a complete representation of the reflective behaviour of the surface of an object due to complex interactions between light and the surface, such as by polarisation, scattering, phosphorescence and fluorescence. For opaque surfaces, the bidirectional reflectance distribution function (BRDF),[14] which is a function of the incident and the reflecting angles of light, is usually employed for colour rendering. However, considering the inconvenience of collecting BRDF data, it is often desirable to perform colour rendering based on two-dimensional images.[15–17] In this section, an image-based colour synthesis technique is presented to modify the colour of three-dimensional object surfaces in a single image so that the colour appearance of the synthesised image is perceptually close to that of the target one. More precisely, given two objects I_1 and I_2 with different surface colours, the purpose is to first recover the intrinsic colour characteristic C_1 and C_2 from I_1 and I_2, respectively, and then map C_2 on to object I_1, so that the colour appearance of the synthesised new object I_1 is very similar to that of I_2. In this technique, the implicit geometric coefficient is calculated

using the least-squares method. Then, the body colour of the three-dimensional objects is recovered using the high correlation between different channels. With the recovered geometric coefficient and the body colour, new images for 3D images can be synthesised. The colour synthesis technique can be applied to a variety of materials that can be described by the dichromatic reflection model.[18] This technique is especially useful for textile products, because of the complicated geometry of their surfaces.

6.5.1 Dichromatic-based modelling of colour reflections

In computer vision, the experiential dichromatic reflection model was first introduced by Shafer to describe light reflection.[18] Figure 6.11 illustrates the interaction between illumination and object surface. When a ray of light strikes the surface of an inhomogeneous material, part of it is reflected from the interface between the object and air immediately because of the difference in the refractive indices of the object and the air. This part of the light is called the surface reflection. The surface reflection is dependent upon the orientation of the local surface that varies along the interface. When the surface is smooth, the surface reflection is very directional, and when the surface has some degree of roughness, the light rays are scattered to some extent around the angle of perfect mirror reflection. In addition to the surface reflection, part of the light penetrates the interface and enters the body of the object, where it keeps hitting the colourants and is scattered by the colourants. The spectral power distribution of the surface reflection is very similar to that of the incident light. The colourants and the medium also absorb part of the light. Part of the scattering light arrives back at the object surface and re-enters the air. This part of the light has been selec-

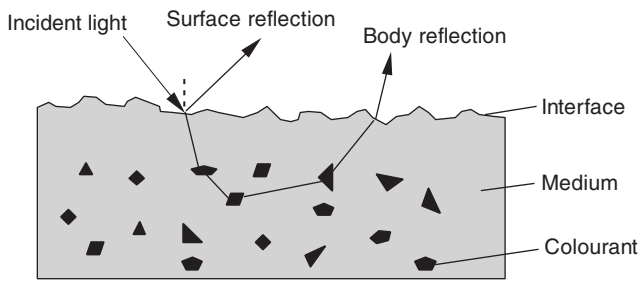

6.11 Reflection from an inhomogeneous surface consists of surface reflection and body reflection.

tively absorbed by the colourants and the medium. It is called body reflection. Based on the dichromatic reflection model, the spectral reflectance $R^p(\lambda)$ at pixel position p can be decomposed into diffuse reflectance $R_b(\lambda)$ and constant surface reflectance R_s:

$$R^p(\lambda) = \alpha^p R_b(\lambda) + \beta^p R_s \quad [6.9]$$

where (α^p,β^p) is the implicit geometric coefficient. Similarly, the RGB output, $\boldsymbol{V}^p$, of an imaging device can be decomposed into diffuse colour, $\boldsymbol{V}_B$, and surface colour, $\boldsymbol{V}_S$:

$$\boldsymbol{V}^p = \alpha^p \boldsymbol{V}_B + \beta^p \boldsymbol{V}_S \quad [6.10]$$

In (6.11), when $\boldsymbol{V}_B$ and $\boldsymbol{V}_S$ are known, the coefficient (α^p,β^p) can be resolved using the least-squares method.

6.5.2 Calculation of body colour

In an imaging system, the illumination colour $\boldsymbol{V}_S$ can easily be obtained by imaging a perfect white patch. Thus, one purpose of colour synthesis is to accurately recover body colour, $\boldsymbol{V}_B$, from images. From (eqn 6.10), the closer the coefficient β^p is to zero, the closer $\boldsymbol{V}^p$ is to $\boldsymbol{V}_B$. The cosine of the including angle θ^p between these two vectors was calculated and then 10% of pixels with large θ^p were selected. For simplicity, $\Re_B$ is used to represent the set of pixels with mainly body colour but little surface colour. The distribution relationship of camera responses between the green and red channel of a red plastic cup in $\Re_B$ is shown in Fig. 6.12.

The point cloud forms a straight line with a high correlation coefficient. Let η_{ij} be the slope between the ith and jth channel. Then the chromaticity of body colour, $\boldsymbol{V}_B$, can be solved as:[19]

$$\boldsymbol{V}_B = \frac{1}{1+\eta_{21}+\eta_{31}}\begin{bmatrix}1\\ \eta_{21}\\ \eta_{31}\end{bmatrix} \quad [6.11]$$

It is noted that (eqn 6.11) does not decide the magnitude of the body colour. For the purpose of colour synthesis, the colour with largest α^p value with respect to the solved $\boldsymbol{V}_B$ was selected as the 'most diffuse' reference colour, $\boldsymbol{V}_{BR}$. As the value of β^p is not considered, the chromaticity of $\boldsymbol{V}_{BR}$ may not be exactly the same as that of the solved $\boldsymbol{V}_B$. However, since $\boldsymbol{V}_{BR}$ is chosen from set $\Re_B$, the surface reflection component of $\boldsymbol{V}_{BR}$ should also be quite small, and therefore it can be used to represent the actual diffuse colour.

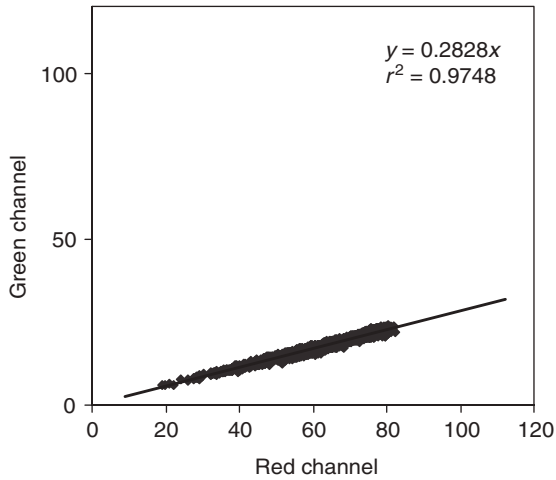

6.12 Distribution of pixel values of green channel with respect to those of red channel in colour set $\Re_B$.

6.5.3 Transform of body colour under different illuminants

In the case of different illuminants, it is necessary to predict the new body colour. This problem falls into the research area of colour constancy.[20,21] The aim of colour constancy is to find a linear transform from colour vector, $\boldsymbol{V}$, under one illuminant to colour vector, $\boldsymbol{V}'$, under another illuminant:[21]

$$\boldsymbol{V}' = \boldsymbol{T}_L \boldsymbol{V} \qquad [6.12]$$

where $\boldsymbol{T}_L$ is a 3×3 illuminant transform matrix. To solve $\boldsymbol{T}_L$, three or more distinct training colours can be used. With the calculated $\boldsymbol{T}_L$, the new body colours under the new illuminant can easily be calculated according to (6.12).

6.5.4 Colour synthesis results and discussion

The process of colour synthesis for three-dimensional objects can be summarised as follows:

1. calculating the diffuse colours of different regions;
2. recovering the geometric coefficient using least-squares method;
3. calculating the new body and surface colours under new a illuminant if necessary;
4. performing colour synthesis.

In the experiment, the imaging device is a QImaging Retiga EXi digital 12-bits monochromatic CCD camera, together with the QImaging RGB liquid crystal colour filter, to acquire colour images. The linearity of the camera was verified by investigating the relationship between the mean reflectance and camera response values of the 20 Kodak Grayscales. To evaluate the colour accuracy of the colour synthesis technique, four plastic cups with the same shape but different colours were used. The implicit geometric coefficient (α^p,β^p) was calculated from one cup and then applied to another cup. The coefficient calculated from the yellow cup is shown in Fig. 6.13 (see also colour section). Table 6.3 shows the mean colour difference, ΔE_{94}*, between the target object and the synthesised object when applying a weighted least-square method. It is found that, in many cases, the colour difference is very small. Large errors occur when applying the coefficients of green and blue cups to synthesise yellow cups. The reason is that the colour in the red channel of these two source cups is much smaller than in that of yellow cup, and thus a small deviation of (α^p,β^p) is enlarged in the colour synthesis process.

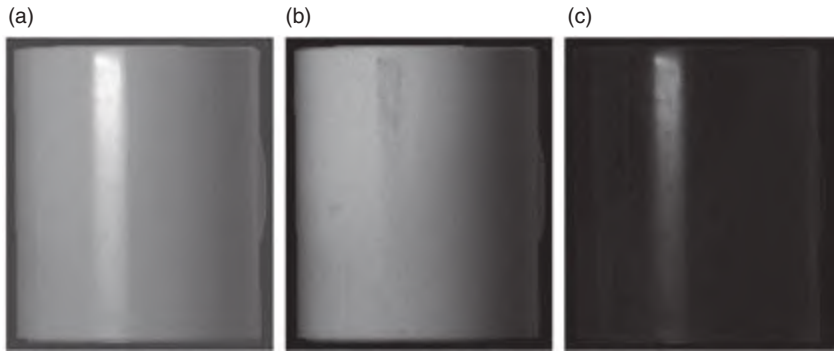

6.13 Calculated geometric coefficient α^p values (b) and β^p values (c) from a colour image (a). The coefficients were rescaled for display.

Table 6.3 Mean colour difference ΔE_{94}* of colour transfer between cups with different colour

		Target cups			
		Red	Green	Blue	Yellow
Source cups	Red	0.441	1.634	1.716	2.844
	Green	2.412	1.240	1.255	4.543
	Blue	2.482	1.190	0.341	5.332
	Yellow	0.814	1.644	1.607	1.833

A light blue filter was used in front of the lens of the camera to produce a new illuminant condition. The illuminant transform matrix, $\boldsymbol{T}_L$, was calculated using the 24 colour patches on MechBetch® ColorChecker® and is given as follows:

$$T_L = \begin{bmatrix} 0.623 & 0.027 & -0.003 \\ -0.006 & 0.745 & 0.013 \\ 0.002 & -0.007 & 0.840 \end{bmatrix} \quad [6.13]$$

The mean colour difference, ΔE_{94}*, between the actual colour and the calculated one using $\boldsymbol{T}_L$ is 0.385. Colour synthesis under the new illuminant is shown in Fig. 6.14 (see also colour section). It can be found that the colour appearances of these two images are quite close.

For multi-coloured objects, image segmentation should be performed before colour synthesis.[19] Then, the body colour of each separated region can be calculated and colour synthesis can be applied to each region. Figure 6.15 (see also colour section) shows the colour synthesis results of some three-dimensional textile products. It is found that the colour appearances of the synthesised images and the target images are very close.

6.6 Future trends and further information

In this chapter a colour mapping algorithm for a two-dimensional texture image of textile fabric is introduced in section 6.2. In section 6.4, a colour synthesis technique for three-dimensional textile products presented. In these two algorithms, colour fidelity is emphasised, because of its impor-

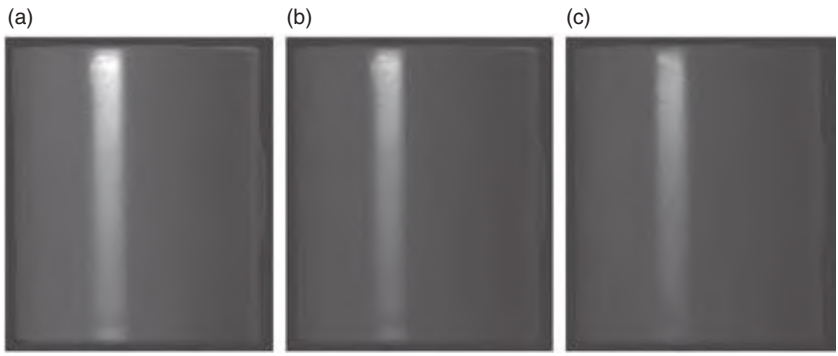

6.14 Colour synthesis results under different illuminant. (a) Original image of blue cup, (b) synthesised image of red cup under new illuminant, (c) actual image of red cup acquired under new illuminant.

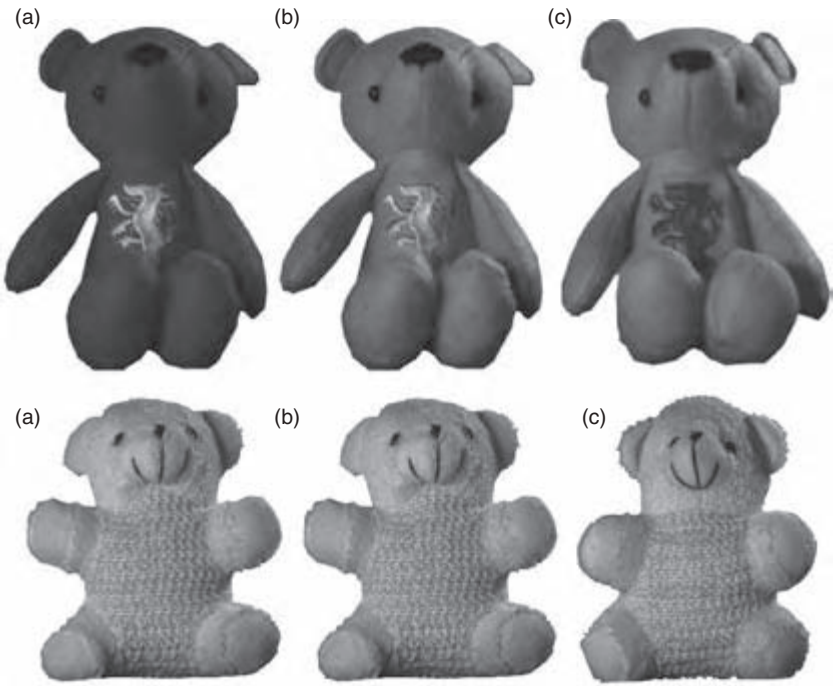

6.15 Synthesised image (b) is produced using the geometric information of original image (a) and the body colour of target image (c).

tance in the textile industry. Based on the colour mapping algorithm, the texture effect on visual colour difference is investigated in section 6.3.

Colour simulation is an active area in computer vision and computer graphics. Recently, new algorithms for colour transfer in grey/colour image/video have been proposed.[7–9,14,17,19,22–24] Of these algorithms, some are based on the physical vision model, while others are based on the statistical characteristics of natural images. Future studies may focus on research areas such as colour fidelity, computational efficiency and reduction of user interaction. With wide applications in multimedia, colour simulation in three-dimensional environments may well be the future direction. The research will, undoubtedly, greatly benefit the visual exhibition of textile garments and interior design.

The visualisation and matching of solid colour on CRT has become a routine process in many textile companies. However, due to the texture pattern on textile fabrics, more efforts should be devoted to the investigation of texture effects on visual colour difference evaluation. One possible future line of research might be to extract additional texture features corresponding to visual properties of texture images. Then, texture features

could be incorporated into colour difference formulae, based on the results of new set of psychophysical experiments.

6.7 References

1. Xin, J.H., Shen, H.L. and Lam C.C. (2005). Investigation of texture effect on visual colour difference evaluation, *Color Research and Application*, **30**, 341–347.
2. Berns, R.S., Motta, R.J. and Gorzynski, M.E. (1993). CRT colorimetry. Part I: theory and practice. *Color Research and Application*, **18**, 299–314.
3. Commission Internationale de l'Eclairage (CIE) (1996). The relationship between digital and colorimetric data for computer-controlled CRT displays, Publication CIE No. 122, Austria: Bureau Central de la CIE.
4. Day, E.A., Taplin, L. and Berns, R.S. (2004). Colorimetric characterization of a computer-controlled liquid crystal display. *Color Research and Application*, **29**, 365–373.
5. Pratt, W.K. (1991). *Digital Image Processing*, 2nd edn. New York: John Wiley & Sons.
6. Botchko, V., Jaaskelainen, T. and Parkkinen, J. (2002). Multispectral texture model for color and highlight reproduction, First European Conference on Colour in Graphics, Image, and Vision, France, 603–607.
7. Montag, E.D. and Berns, R.S. (2000). Lightness dependencies and the effect of texture on suprathreshold lightness tolerances. *Color Research and Application*, **25**, 241–249.
8. Shen, H.L. and Xin, J.H. (2004). Dichromatic based rendering of texture image with high colour fidelity. *Journal of Imaging Science and Technology*, **48**, 246–250.
9. Xin, J.H. and Shen, H.L. (2004). Recolouring digital textile printing design with high fidelity. *Coloration Technology*, **120**, 6–13.
10. Fairchild, M.D. (1998). *Color Appearance Models*. Reading, MA: Addison–Wesley.
11. Xin, J.H., Lam, C.C. and Luo, M.R. (2001). Investigation of parametric effects using medium colour difference pairs. *Color Research and Application*, **26**, 376–383.
12. International Standard ISO 105-A02 (1993). Textiles – tests for colour fastness – Part A02: Grey scale for assessing change in colour.
13. Guan, S.S. and Luo, M.R. (1999). Investigation of parametric effects using small colour difference. *Color Research and Application*, **24**, 331–343.
14. Nicodemus, F.E., Richmond, J.C., Hsia, J.J., Ginsberg, I.W. and Limperis, T. (1997). Geometric considerations and nomenclature for reflectance, US Department of Commerce, National Bureau of Standards, Monograph 160.
15. Reinhard, E., Ashikhmin, M., Gooch, B. and Shirley, P. (2001). Color transfer between images. *IEEE Computer Graphics and Applications*, **21**, 34–41.
16. Peng, L. (1998). Dichromatic based photographic modification. Proceedings of the Sixth Color Imaging Conference, 96–99.
17. Xin, J.H. and Shen, H.L. (2004). Accurate color synthesis of three-dimensional objects in an image. *Journal of the Optical Society of America A*, **21**, 713–722.

18. Shafer, S.A. (1985). Using color to separate reflection components. *Color Research and Application*, **10**, 210–218.
19. Shen, H.L. and Xin, J.H. (2005). Transferring colors between three-dimensional objects. *Applied Optics*, **44**, 1969–1976.
20. Barnard, K., Cardei, V. and Funt, B. (2002). A comparison of computational color constancy algorithms – Part I: methodology and experiments with synthesized data. *IEEE Transactions on Image Processing*, **11**, 972–983.
21. Finlayson, G.D., Drew, M.S. and Funt, B.V. (1994). Color constancy: generalized diagonal transforms suffice. *Journal of the Optical Society of America A*, **11**, 3011–3019.
22. Xin, J.H. and Shen, H.L. (2003). Computational model for color mapping on texture images. *Journal of Electronic Imaging*, **12**, 697–704.
23. Welsh, T., Ashikhmin, M. and Mueller, K. (2002). Transferring color to grayscale images. *ACM Transactions on Graphics*, **20**, 277–280.
24. Levin, A., Lischinski, D. and Weiss, Y. (2004). Colorization using optimization, *ACM Transactions on Graphics*, **23**, 689–694.